



Hierarchical Nanostructured TiO₂ Films Prepared by Reactive Pulsed Laser Deposition for Photoelectrochemical Water Splitting

Roberto Matarrese^a, Isabella Nova^{*a}, Andrea Li Bassi^b, Carlo S. Casari^b, Valeria Russo^b

^aLaboratory of Catalysis and Catalytic Processes, Dipartimento di Energia, Politecnico di Milano, P.zza L. da Vinci 32, 20133, Milano, Italy

^bMicro- and Nanostructured Materials Lab., Dipartimento di Energia, Politecnico di Milano; via Ponzio 34/3, 20133 Milano, Italy
 isabella.nova@polimi.it

Hierarchical tree-like TiO₂ nanostructures prepared by PLD are proposed as photoanodes for photoelectrochemical water splitting. The structural/morphological properties of the TiO₂ nanostructures have been tuned via a fine control of the growth parameters (e.g., background gas pressure), of the mass of catalyst, and of the annealing treatments. A correlation between structural/morphological properties and photoelectrochemical behaviour was found. The best performances were associated with the sample prepared at 5Pa of oxygen, possibly because optimized values of density/surface area, crystallinity and electron transport are achieved. The effect of the variation in the mass of deposited material, which leads to an increased thickness of the catalytic layers, clearly shows the existence of an optimal thickness value that can guarantee improved electron transfer. Thermal annealing at 650°C resulted in an increased degree of crystallinity which positive affects the photoelectrochemical response.

1. Introduction

Since Fujishima and Honda (1972) reported for the first time the photoelectrochemical (PEC) water splitting into H₂ and O₂ over TiO₂ anodes, a lot of investigation has been dedicated to the production of hydrogen from water and solar energy, for its potential to provide a clean and renewable energy resource (Bak et al., 2002). Many other materials have been considered in PEC applications, but TiO₂ still remains the most widely investigated photocatalyst in consideration of its high activity, chemical inertness, low cost and non toxicity.

In the last years, nanostructured TiO₂ architectures and in particular nanotubes (Mor et al., 2006; Macak et al., 2007), have attracted increasing interest due to their highly ordered structure and the facile control of size. In particular, the vertically oriented, immobilised and high-aspect ratio nanotubes are considered smart structures for photo-induced processes, as they improve the electron transport properties and provide longer electron lifetime, possibly by lowering the electron-hole (e-h) recombination which plays crucial role in photocatalytic reactions.

More recently, novel quasi 1-D hierarchical structures received attention for their advantages in combining large surface area, light scattering potential and anisotropic morphology (similarly to nanotubes) to ensure better electron transport (Di Fonzo et al., 2009). In particular, nanocrystalline tree-like TiO₂ hierarchical microstructures prepared by reactive pulsed laser deposition (PLD) have been recently proposed for application in dye-sensitized solar cells showing longer electron lifetime, high performances for ionic liquid electrolytes diffusion and strong light trapping capability (Sauvage et al., 2010, Passoni et al., 2013). Moreover, the potential photocatalytic efficiency of such hierarchical TiO₂ architectures has been proved in the mineralization (i.e. oxidation) of stearic acid, as a model molecule (Di Fonzo et al., 2009).

In this work, we discuss the use of hierarchical tree-like assemblies of TiO₂ nanoparticles obtained by Pulsed Laser Deposition (PLD) as photoanodes for the photoelectrochemical water splitting process. In particular, the effect of the preparation conditions (i.e. PLD parameters and annealing temperature) on the crystalline structure and morphology of the obtained titanium oxide films and the consequent impact on the photoelectrochemical response, have been investigated.

2. Materials and Methods

2.1 Synthesis of TiO₂ hierarchical photoanodes

TiO₂ hierarchically structured films have been deposited by ablation of a TiO₂ target with UV ($\lambda=266$ nm) laser pulses from a frequency quadrupled Nd:YAG laser, with pulse duration about 5-7 ns. The laser fluence on the target was about 2.5 J/cm² with a spot size of about 3 mm². The ablation was performed in the presence of a background gas pressure of pure oxygen (99.999%) in the 3-10 Pa range. Silicon, glass and Ti were used as substrates mounted on an off-axis rotating sample holder at a fixed target-to-substrate distance of 50 mm. Ti plate substrates for photoelectrochemical measurements were masked to deposit on a 2x1 cm² area and to leave a clean surface for electrical contacts. All the depositions were performed with substrates kept at room temperature and no significant heating was observed during deposition. The deposited mass was estimated by a quartz crystal microbalance at the same position as the substrates. Since the deposition rate changes depending on the background gas pressure, films were deposited with a constant mass per unit surface of 0.5M (about 0.15-0.2 mg/cm²), and of M and 2M for the films deposited at 5 Pa, in order to address the role of mass/thickness. Post deposition thermal annealing was performed for 2 hours in air in a muffle furnace at 500°C, 650°C at 800 °C to induce transition to crystalline TiO₂, as discussed below.

2.2 Characterization

SEM analyses were performed on TiO₂ on silicon substrates with a ZEISS Supra 40 FEG-SEM without any sample preparation. Film density was evaluated by combining information on the deposited mass with thickness measurements by cross-sectional SEM images. Raman spectra were measured on TiO₂ on glass/silicon with a Renishaw InVia micro Raman spectrometer with 514.5 nm laser excitation wavelength.

2.3 Photoelectrochemical experiments

The photoelectrochemical water splitting behaviour was investigated in aqueous KOH solution (0.1 M) with a three-electrodes configuration consisting of a TiO₂ photo-anode (nominally 1 cm²) as the working electrode, a platinum grid as the counter electrode and a saturated calomel electrode (SCE) as the reference. Of note all the values of potential in the text are referred to SCE. The external bias was provided by a potentiostat (Amel 7050) with potential ramps from OCV to about 0.5 V, with a scan rate of 5 mV/s. The light source was a tungsten filament and a high-pressure lamp (Osram Ultra-Vitalux lamp, 300 W). An average UVA/UVB light intensity, striking on the electrodes surface, of about 1350 μ W/cm² was measured by a light meter HD2302.0 (Delta OHM).

3. Results and discussion

3.1 Photoanodes structure and morphology

In Figure 1, SEM cross section images of as-deposited samples obtained at different O₂ background pressures (i.e. 3, 5 and 10Pa, respectively) keeping the total deposited mass per unit surface constant (0.5M) are shown. Of note, the same scale bar outlines the change in porosity and film thickness. We observe that a gradual variation of film morphology from compact/columnar towards a nanoporous assembly occurs when deposition pressure changes from 3Pa to 10Pa. In particular, at 3Pa O₂ (Figure 1A) a compact and dense film develops while starting from 5Pa O₂ (Figure 1B), hierarchical structures resembling a forest of nano-trees are obtained. As discussed in detail in previous works (Bailini et al., 2007; Di Fonzo et al., 2009), the gas pressure strongly affects the growth mechanisms, since the presence of a background atmosphere induces nucleation of the ablated species leading to the formation of clusters that are subsequently slowed down after diffusion in the background gas. This corresponds to a change in the growth mechanisms from atom-by-atom deposition in vacuum (leading to dense films) to low energy cluster assembling at higher pressures (resulting in the deposition of a nanoporous assembly). Since the same mass per unit surface (0.5M) was deposited for all samples grown at different pressures, the film thickness increased from about 500 nm to ca. 2.6 μ m moving from 3 to 10Pa O₂ pressure, corresponding to a decrease in the material density from 3.2 g/cm³ to about 0.7 g/cm³. The corresponding estimated

porosity, expressed in percentage of voids and evaluated from the ratio between film density and bulk anatase density (ca. 3.9 g/cm^3), increases from 18% at 3Pa O_2 to about 83% at 10Pa O_2 .

SEM analyses were also performed for samples deposited by varying mass surface density in the 0.5M-2M range (not reported), showing a corresponding thickness increase from about 900 nm to about 3600 nm.

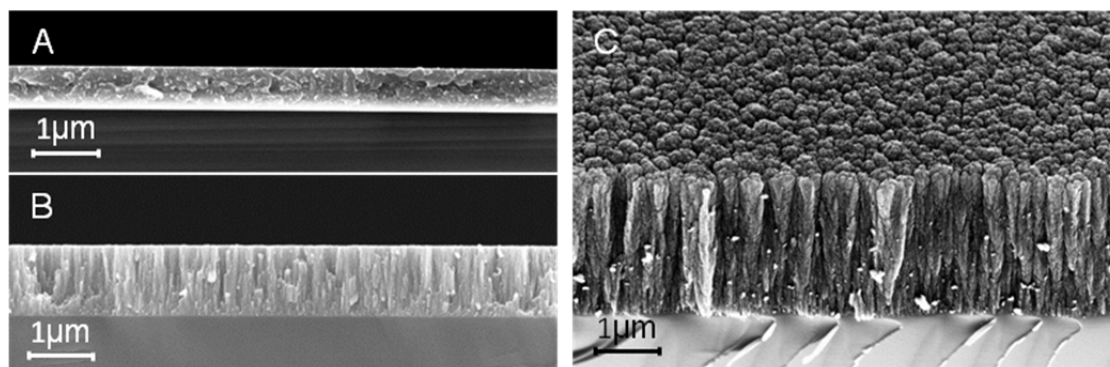


Figure 1: SEM cross sectional images of as-deposited films obtained at oxygen partial pressures of (A) 3Pa, (B) 5Pa, (C) 10Pa.

Figure 2 shows SEM images of samples deposited at 5 Pa O_2 and annealed in air for 2 hours at 500°C, 650°C and 800°C, respectively. Notably, the thermal treatment does not change the overall morphology of the structures up to 650°C. The crystallization process mainly affects the shape of single nanoparticles and leads to a sintering effect, with increased coalescence and thus connectivity among nanoparticles. At the highest annealing temperature, Figure 2C, the occurrence of a strong coalescence leading to quasi 1-D columnar structure with an evident decrease in porosity, is observed.

The crystalline structure of the films was characterized by Raman spectroscopy (results not reported) that is sensitive to the local crystalline order/disorder and provides a fingerprint of the TiO_2 crystalline phase (Li Bassi et al., 2005). As expected, all as-deposited films show an amorphous structure as a result of the room temperature growth process, while thermal annealing in air induces transition to a crystalline structure, i.e. anatase TiO_2 . No substantial differences in the Raman spectra were observed for samples grown at different pressures, both for as-deposited films and after annealing, up to 5Pa. Only for films deposited at higher pressure (10Pa) the presence a small fraction of rutile phase was observed after annealing at 500°C and higher T. This oxide phase evolution as a consequence of annealing is in agreement with previous XRD and Raman characterizations of TiO_2 films grown under similar conditions (Di Fonzo et al., 2009).

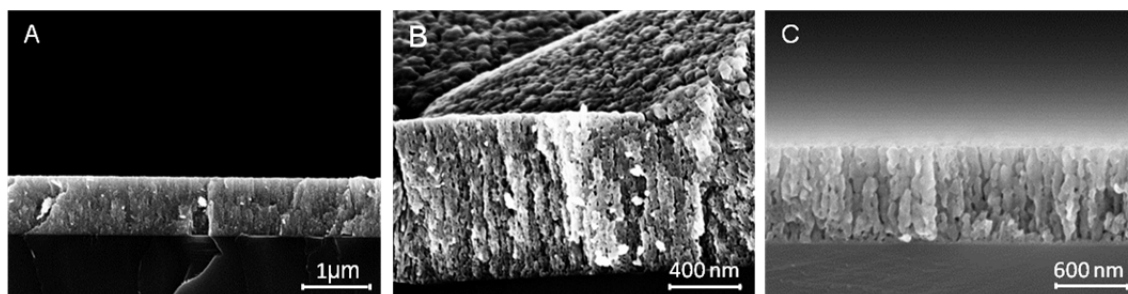


Figure 2: SEM cross sectional images of TiO_2 deposited at 5 Pa O_2 and annealed in air at (A) 500°C, (B) 650°C and (C) 800°C.

3.2 Photoelectrochemical response

The photoelectrochemical behaviour of TiO₂ photoanodes produced at different deposition pressures (keeping the total deposited mass per unit surface constant (0.5M)) and annealed at 500°C, is shown in Figure 3A. For comparison purpose a typical result obtained under dark condition is also reported.

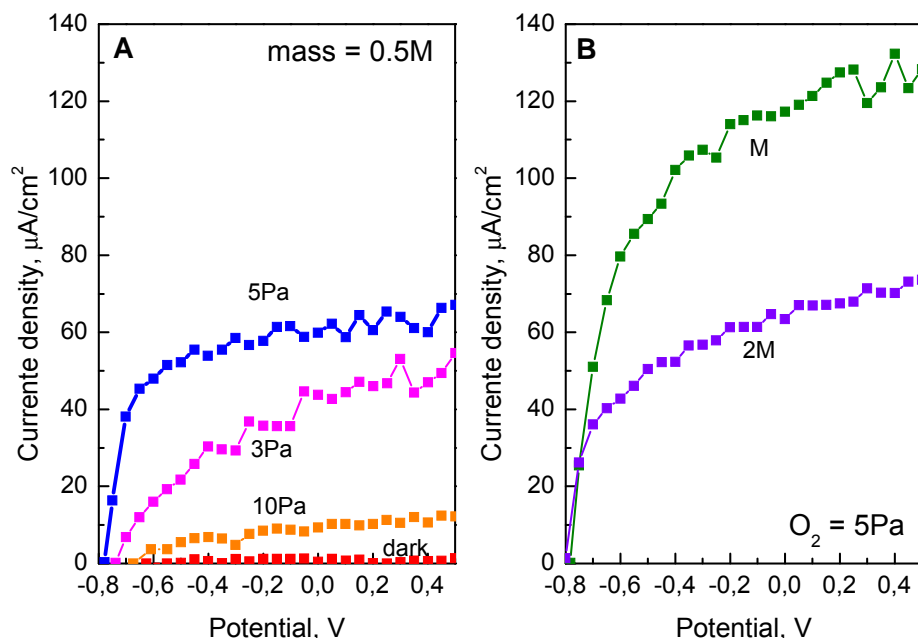


Figure 3: Current-potential responses in 0.1M KOH solution in the dark and under illumination: (A) TiO₂ photoanodes produced at different background pressure keeping the mass surface density constant (0.5M); (B) TiO₂ photoanodes produced at 5Pa O₂ by varying the mass surface density. All the samples were annealed at 500°C.

Notably, nearly no current can be observed within the entire potential sweep range without illumination, indicating that no photoelectrochemical water splitting occurred at the anodes surface in the dark. On the contrary, upon illumination, water splitting photocurrent was observed over all the investigated samples. Results clearly show that the best performances are associated with the sample prepared at 5Pa which shows higher photocurrent density in the whole potential range, e.g. reaching a near-constant value of ca. 65 µA/cm² at 0.5V. The lowest photoresponse is observed for the sample deposited at the highest oxygen pressure (10Pa) while an intermediate behaviour is observed at 3Pa oxygen.

To rationalize these trends, the morphology of the different samples grown in the 3-10Pa range has to be considered. As discussed above, the background atmosphere strongly affects the TiO₂ film growth mechanisms and its final porosity. In particular, an increase in the deposition pressure corresponds to an increase in porosity and thus in the available active surface area (as discussed in Passoni et al., 2013). As a matter of facts, at the lowest pressure (3Pa) a dense and compact film develops while at higher deposition pressures (5-10Pa) a tree-like hierarchical organization is obtained. On the other hand, the increased deposition pressure leads to a parallel decrease in film density. On this basis, it is not surprising that the sample deposited at 5Pa O₂, for which a specific surface area of about 23 m²/g was measured by dedicated BET analysis, shows a much better photoactivity than the compact sample at 3Pa. However, as deposition pressure is increased up to 10Pa, porosity and thus film thickness increase, and it may be argued that this could negatively affect the electrical transport properties of the material as a consequence of the excessive length of the electron path. Moreover, the change from a columnar tree-like morphology towards a more open structure could imply higher recombination losses, leading to a significant photoresponse decrease for the sample deposited at 10Pa.

In order to gain more information on this aspect, the effect of optimal TiO₂ photoanode morphologies (5 Pa) when varying the mass of deposited material, and hence the effect of film thickness and of total surface area, on the photoelectrochemical behaviour, was analysed. Figure 3B shows the photoelectrochemical results obtained for samples deposited by increasing mass surface density up to M

and 2M. In this case, all films were deposited at the same oxygen pressure (i.e. 5Pa) and annealed in air at the same temperature (i.e. 500°C.).

A clear effect of the deposited mass on the photoresponse is apparent: in particular, mass-M sample yields to a maximum photocurrent density close to 120 $\mu\text{A}/\text{cm}^2$ at 0.5V, which is about 2 times higher than that of mass-0.5M sample (Figure 3A vs. 3B). Besides, when the mass is increased up to 2M, the photoresponse decreases significantly. These results likely suggest the existence of an optimal thickness value that can guarantee improved electron transfer. Moreover, electrolyte mass-transport limitations could explain the lower performances observed for the longer hierarchical treelike structures.

Finally, the effect of the post-thermal treatment on the photoresponse was investigated. For this purpose, photoelectrochemical experiments were performed on TiO_2 photoanodes prepared at 5Pa oxygen with 0.5M mass and annealed at 500, 650 and 800°C. The results are shown in Figure 4A. It is evident that the sample annealed at 650°C shows the best performances over the whole potential range. In particular, the photocurrent density reaches a value of about 200 $\mu\text{A}/\text{cm}^2$ at 0.5V which is nearly tripled if compared to that of sample annealed at 500°C. Conversely, the photoresponse is almost totally suppressed after annealing samples at 800°C.

The corresponding overall photoconversion efficiency ($\eta\%$) was calculated according to the following Eq.(1) (Varghese et al., 2008), which takes into account not only the power light but also the external potential applied to the electrode:

$$\eta (\%) = (I_p (1.229 - |V|) / J) * 100 \quad (1)$$

where, I_p is the photocurrent density ($\mu\text{A}/\text{cm}^2$), 1.229 (V) is the standard reversible potential for the overall water splitting reaction, $|V|$ is the applied potential evaluated as the difference between the bias potential and the OCV under the irradiated power light, and J is the overall UV incident light power density of about 1350 $\mu\text{W}/\text{cm}^2$. Figure 4B shows the variation of $\eta\%$ as a function of the applied potential.

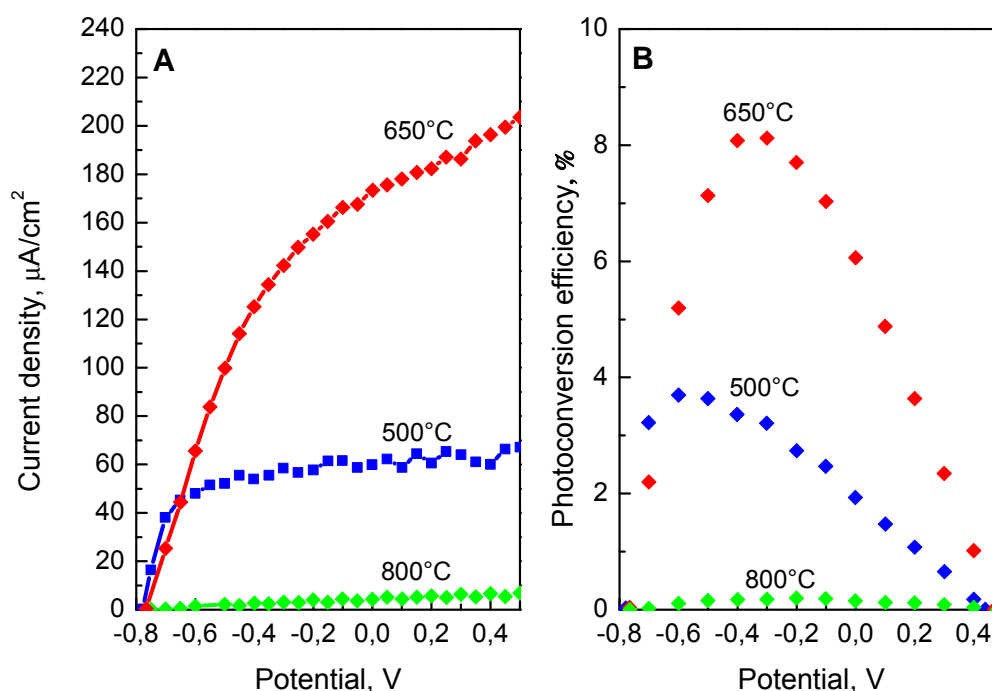


Figure 4: Current-potential responses in 0.1M KOH solution under illumination: (A) TiO_2 photoanodes produced at 5Pa O_2 with 0.5M by varying the annealing temperature. (B) Photoconversion efficiency as a function of the applied potential.

It clearly appears that the sample annealed at 650°C achieves the highest efficiency of ca. 8.1% at -0.3 V.

The result can be explained by considering the effect of the thermal treatment on the samples morphology. As previously discussed, the temperature increase from 500°C to 650°C induces moderate sintering/densification of the tree like structures, which seems to be better defined for the sample calcined at 650°C. Accordingly, the reduced crystalline defectivity obtained by annealing samples at 650°C should enhance the charge transfer and electron conductivity of TiO₂ films. On the other hand the further increase in the annealing temperature up to 800°C showed a high coalescence degree occurring within the tree like structures (e.g. leading to the decrease of specific surface area) which, most likely, is the cause for the observed decrease in the photoresponse.

4. Conclusions

In this paper we have presented a photoelectrochemical characterization of hierarchical nanostructured TiO₂ layers prepared by Pulsed Laser Deposition, with the potential to be employed for the water splitting production of hydrogen. Open morphologies characterized by a relevant porosity and a tree-like, quasi-1D morphology have shown promising results achieving photocurrent values up to 200 $\mu\text{A}/\text{cm}^2$ and efficiency up to 8%. The observed trends in photocurrent have been discussed as a function of the post-deposition thermal treatment, of the material morphology and of the layer thickness, showing optimal values which were attributed to a balance between available surface area and electron transport/recombination related to the crystallinity and connectivity of the structure. Future work will focus on the optimization of the material structure-morphology and on possible routes for enhancing the response to visible light (e.g. doping, sensitization).

References

- Bailini A., Di Fonzo F., Fusi M., Casari C.S., Li Bassi A., Russo V., Baserga A., Bottani C.E., 2007, Pulsed laser deposition of tungsten and tungsten oxide thin films with tailored structure at the nano- and mesoscale, *Applied Surface Science* 253, 8130-8135.
- Bak T., Nowotny J., Rekas M., Sorrell C.C., 2002, Photo-electrochemical hydrogen generation from water using solar energy. Materials-related aspects, *International Journal of Hydrogen Energy* 27, 991-1022.
- Di Fonzo F., Casari C.S., Russo V., Brunella M.F., Li Bassi A., Bottani C.E., 2009, Hierarchically organized nanostructured TiO₂ for photocatalysis applications, *Nanotechnology* 20, 015604, 1-7.
- Fujishima A., Honda K., 1972, Electrochemical Photolysis of Water at a Semiconductor Electrode, *Nature* 238, 37-38.
- Li Bassi A., Cattaneo D., Russo V., Bottani C.E., Barborini E., Mazza T., Piseri P., Milani P., Ernst F.O., Wegner K., Pratsinis S.E., 2005, Raman spectroscopy characterization of titania nanoparticles produced by flame pyrolysis: The influence of size and stoichiometry, *Journal of Applied Physics* 98, 074305, 1-9.
- Macak J.M., Tsuchiya H., Ghicov A., Yasuda K., Hahn R., Bauer S., Schmuki P., 2007, TiO₂ nanotubes: Self-organized electrochemical formation, properties and applications, *Current Opinion in Solid State and Materials Science* 11, 3-18.
- Mor G.K., Varghese O.K., Paulose M., Shankar K., Grimes C.A., 2006, Review on highly ordered, vertically oriented TiO₂ nanotube arrays: Fabrication, material properties, and solar energy applications, *Solar Energy Materials & Solar Cells* 90, 2011-2075.
- Passoni L., Ghods F., Docampo P., Abrusci A., Marti-Rujas J., Ghidelli M., Divitini G., Ducati C., Binda M., Guarnera S., Li Bassi A., Casari C.S., Snaith H.J., Petrozza A., Di Fonzo F., 2013, Hyperbranched Quasi-1D Nanostructures for Solid-State Dye-Sensitized Solar Cells, *ACS Nano* 7 (11), 10023-10031.
- Sauvage F., Di Fonzo F., Li Bassi A., Casari C.S., Russo V., Divitini G., Ducati C., Bottani C.E., Comte P., Graetzel M., 2010, Hierarchical TiO₂ photo-anode for dye-sensitized solar cells, *NanoLetters* 10, 2562-2567.
- Varghese O.K., Grimes C.A., 2008, Appropriate strategies for determining the photoconversion efficiency of water photoelectrolysis cells: a review with examples using titania nanotube array photoanodes. *Solar Energy Mater Solar Cells* 92, 374-384.